Experimental tripartite quantum state sharing and perfect teleportation of the two-qubit photonic state using genuinely entangled multipartite states

Parminder S. Bhatia

Research Laboratory of Electronics, Massachusetts Institute of Technology, Cambridge, Massachusetts 02139, USA (psbhatia20002@gmail.com)

Received June 11, 2013; revised November 20, 2013; accepted November 27, 2013; posted December 2, 2013 (Doc. ID 192093); published December 23, 2013

An experimental scheme, its hardware implementation, and procedure for experimental verification of tripartite quantum state sharing and perfect teleportation of the two-qubit photonic state using four different multipartite quantum channels is presented. The four multipartite channels considered are (1) a pair of Greenberger–Horne–Zeilinger triplets, (2) a six-particle cluster state, (3) a highly entangled five-particle Brown state, and (4) a highly entangled six-particle Borras state. In this experiment, optical pulses are delivered by a high repetition rate mode-locked pulsed laser and arbitrary photonic states, in the two-qubit Bloch sphere, are created by the spontaneous parametric down-conversion of optical pulses in a nonlinear crystal. The experimental implementation of the scheme is based on both single-particle and two-particle complete Bell-state measurements, and the unitary transformation required for reconstruction of the qubit is performed using single- and two-qubit operations. Two-qubit operations are implemented using the quantum controlled phase and C-NOT gates. Relative comparison among different multipartite channels along with experimental difficulties and their solutions are also discussed. © 2013 Optical Society of America

OCIS codes: (190.4410) Nonlinear optics, parametric processes; (320.2250) Femtosecond phenomena; (270.5565) Quantum communications; (270.5585) Quantum information and processing.
http://dx.doi.org/10.1364/JOSAB.31.000154

1. INTRODUCTION

Tripartite-controlled teleportation of a single-qubit using a three-particle Greenberger–Horne–Zeilinger (GHZ) triplet was earlier studied in [1], while the quantum state sharing (QSTS) and perfect teleportation of an arbitrary two-qubit state using different multipartite quantum channels was first theoretically treated in the series of papers, which can be found in [2–4]. However, most of this theoretical study using multipartite channels relies on three- and four-particle measurements, which with the existing quantum information technology cannot be realized in the experiment. Later, simplified versions, which was based on single-particle and two-particle measurements, of the above stated theoretical work on QSTS and teleportation of two-qubit state was addressed in separate publications [5,6]. To the best of our knowledge, on QSTS and teleportation of two-qubit state using multipartite quantum channels, no experiment has yet been reported. In this paper, we present experimental schemes, their hardware implementation, and experimental procedure for QSTS and perfect teleportation of an arbitrary two-qubit photonic state using four different multipartite quantum channels, which are: (1) a pair of GHZ triplets [7], (2) a six-particle cluster state [8], (3) a five-particle Brown state [9], and (4) a six-particle Borras state [10]. Our experimental schemes and their implementations are based on single-particle and two-particle Bell-state measurements. This paper is organized as follows. In Section 2, schemes for tripartite QSTS and perfect teleportation of an arbitrary two-qubit photonic state using four different multipartite quantum channels are presented. Section 3 deals with the full experimental implementation of the schemes presented in Section 2. In Section 4, relative comparisons among four different multipartite channels and major experimental difficulties are discussed. Section 5 provides the concluding remarks.

2. TRIPARTITE SCHEMES FOR QSTS AND TELEPORTATION OF THE TWO-QUBIT STATE

Our tripartite teleportation system consists of three parties, who are Alice, Bob, and Charlie. These three parties are located at different locations and are connected by classical channels. An arbitrary two-qubit state $|\psi_{12}\rangle = \alpha|0\rangle_1|0\rangle_2 + \beta|0\rangle_1|1\rangle_2 + \gamma|1\rangle_1|0\rangle_2 + \delta|1\rangle_1|1\rangle_2$ is the state to be teleported from Alice to Charlie, where $|\alpha|^2 + |\beta|^2 + |\gamma|^2 + |\delta|^2 = 1$. For the entanglement resource to our tripartite system we consider four different multipartite quantum channels, which are: (1) a pair of GHZ triplets, (2) a cluster state, (3) a Brown state, and (4) a Borras state. These channels are, respectively, given by Eqs. (1)–(4)

$$|\psi_{345}\rangle_{\mathrm{GHZ}} = \frac{1}{\sqrt{2}}\{|0\rangle_3|0\rangle_4|0\rangle_5 + |1\rangle_3|1\rangle_4|1\rangle_5\} \quad \text{and}$$
$$|\psi_{678}\rangle_{\mathrm{GHZ}} = \frac{1}{\sqrt{2}}\{|0\rangle_6|0\rangle_7|0\rangle_8 + |1\rangle_6|1\rangle_7|1\rangle_8\}, \tag{1}$$

 © 2014 Optical Society of America

$$|C_6\rangle = \frac{1}{2}\{+|0\rangle_3|0\rangle_4|0\rangle_5|0\rangle_6|0\rangle_7|0\rangle_8 + |0\rangle_3|0\rangle_4|0\rangle_5|1\rangle_6|1\rangle_7|1\rangle_8 + |1\rangle_3|1\rangle_4|1\rangle_5|0\rangle_6|0\rangle_7|0\rangle_8 - |1\rangle_3|1\rangle_4|1\rangle_5|1\rangle_6|1\rangle_7|1\rangle_8\}, \quad (2)$$

$$|\psi_5\rangle = \frac{1}{2}\{+|0\rangle_3|0\rangle_4|1\rangle_5|\psi_{67}^{(-)}\rangle + |0\rangle_3|1\rangle_4|0\rangle_5|\phi_{67}^{(-)}\rangle + |1\rangle_3|0\rangle_4|0\rangle_5|\psi_{67}^{(+)}\rangle + |1\rangle_3|1\rangle_4|1\rangle_5|\phi_{67}^{(+)}\rangle\}, \quad (3)$$

where $\varphi_{lm}^{(\pm)} = (1/\sqrt{2})\{|0\rangle_l|0\rangle_m \pm |1\rangle_l|1\rangle_m\}$ and $\psi_{lm}^{(\pm)} = (1/\sqrt{2})\{|0\rangle_l|1\rangle_m \pm |1\rangle_l|0\rangle_m\}$. Labels l and m indicate two particles entangled with Einstein–Podolsky–Rosen (EPR) correlation.

earlier in this section. Each of these four states can occur with equal likely probability of 1/4. Figure 2(A) shows the switching of entanglement among eight GHZ particles during a given teleportation trial. Figure 2(B) shows the corresponding case for the eight cluster state particles. The switching of entanglement among seven Brown- and eight Borras-state particles can similarly be drawn. Figure 2(A1) depicts that before the first Bell-state measurement the composite qubit, the first GHZ triplet, and the second GHZ triplet are independent quantum systems. Likewise, Fig. 2(B1) depicts that the composite qubit and the cluster of six qubits are independent. Figure 2(A2) shows that after first Bell-state measurement particles 3, 4, and 5 are no more entangled with the GHZ

$$|\psi_6\rangle = \frac{1}{\sqrt{32}}\left\{\begin{array}{l} +|0\rangle_3|0\rangle_4|0\rangle_5|0\rangle_6|0\rangle_7|0\rangle_8 + |1\rangle_3|1\rangle_4|1\rangle_5|1\rangle_6|1\rangle_7|1\rangle_8 + |0\rangle_3|0\rangle_4|0\rangle_5|0\rangle_6|1\rangle_7|1\rangle_8 + |1\rangle_3|1\rangle_4|1\rangle_5|1\rangle_6|0\rangle_7|0\rangle_8 \\ +|0\rangle_3|0\rangle_4|0\rangle_5|1\rangle_6|0\rangle_7|1\rangle_8 + |1\rangle_3|1\rangle_4|1\rangle_5|0\rangle_6|1\rangle_7|0\rangle_8 + |0\rangle_3|0\rangle_4|0\rangle_5|1\rangle_6|1\rangle_7|0\rangle_8 + |1\rangle_3|1\rangle_4|1\rangle_5|0\rangle_6|0\rangle_7|1\rangle_8 \\ +|0\rangle_3|0\rangle_4|1\rangle_5|0\rangle_6|0\rangle_7|1\rangle_8 + |1\rangle_3|1\rangle_4|0\rangle_5|1\rangle_6|1\rangle_7|0\rangle_8 + |0\rangle_3|0\rangle_4|1\rangle_5|1\rangle_6|1\rangle_7|1\rangle_8 + |1\rangle_3|1\rangle_4|0\rangle_5|0\rangle_6|0\rangle_7|0\rangle_8 \\ +|0\rangle_3|1\rangle_4|0\rangle_5|0\rangle_6|0\rangle_7|1\rangle_8 + |1\rangle_3|0\rangle_4|1\rangle_5|1\rangle_6|1\rangle_7|0\rangle_8 + |0\rangle_3|1\rangle_4|0\rangle_5|0\rangle_6|1\rangle_7|0\rangle_8 + |1\rangle_3|0\rangle_4|1\rangle_5|1\rangle_6|0\rangle_7|1\rangle_8 \\ +|0\rangle_3|1\rangle_4|1\rangle_5|0\rangle_6|0\rangle_7|0\rangle_8 + |1\rangle_3|0\rangle_4|0\rangle_5|1\rangle_6|1\rangle_7|1\rangle_8 + |0\rangle_3|1\rangle_4|1\rangle_5|1\rangle_6|0\rangle_7|1\rangle_8 + |1\rangle_3|0\rangle_4|0\rangle_5|0\rangle_6|1\rangle_7|0\rangle_8 \\ -|0\rangle_3|0\rangle_4|1\rangle_5|0\rangle_6|1\rangle_7|0\rangle_8 - |1\rangle_3|1\rangle_4|0\rangle_5|1\rangle_6|0\rangle_7|1\rangle_8 - |0\rangle_3|0\rangle_4|1\rangle_5|1\rangle_6|0\rangle_7|0\rangle_8 - |1\rangle_3|1\rangle_4|0\rangle_5|0\rangle_6|1\rangle_7|1\rangle_8 \\ -|0\rangle_3|1\rangle_4|0\rangle_5|1\rangle_6|0\rangle_7|0\rangle_8 - |1\rangle_3|0\rangle_4|1\rangle_5|0\rangle_6|1\rangle_7|1\rangle_8 - |0\rangle_3|1\rangle_4|0\rangle_5|1\rangle_6|1\rangle_7|1\rangle_8 - |1\rangle_3|0\rangle_4|1\rangle_5|0\rangle_6|0\rangle_7|0\rangle_8 \\ -|0\rangle_3|1\rangle_4|1\rangle_5|0\rangle_6|1\rangle_7|1\rangle_8 - |1\rangle_3|0\rangle_4|0\rangle_5|1\rangle_6|0\rangle_7|0\rangle_8 - |0\rangle_3|1\rangle_4|1\rangle_5|1\rangle_6|1\rangle_7|0\rangle_8 - |1\rangle_3|0\rangle_4|0\rangle_5|0\rangle_6|0\rangle_7|1\rangle_8 \end{array}\right\}. \quad (4)$$

The tripartite scheme for the teleportation of the two-qubit state from Alice to Charlie using the GHZ channel is shown in Fig. 1(A). In this figure, the dotted line between particles indicates the entanglement between them. With the additional dotted line between particles 4 and 7, Fig. 1(A) also depicts the tripartite teleportation scheme for the cluster state channel. Figures 1(B) and 1(C) depict the tripartite teleportation scheme using Brown and Borras channels, respectively. Four steps required to practice perfect teleportation from Alice to Charlie are discussed below.

Step 1. For all four multipartite channels, the first Bell-state measurement (BSM-1) is made on the same two particles, which are particles 1 and 3. As a result of this measurement, particles 1 and 3 can be projected into one of the four EPR Bell-states denoted by $\varphi_{13}^{(\pm)}$, $\psi_{13}^{(\pm)}$, which were defined

quantum correlation, particles 1 and 3 are projected into the EPR Bell-state, and particles 2, 4, and 5 get entangled. Likewise, Fig. 2(B2) shows that after first Bell-state measurement particle 3 is no longer a part of the cluster state, particles 1 and 3 are projected into the EPR Bell-state, and particles 2, 4, 5, 6, 7, and 8 get entangled.

Step 2. We next make a second Bell-state measurement (BSM-2). For GHZ- and cluster-state channels this measurement is made on particles 2 and 6 while for Brown- and Borras-state channels it is made on particles 2 and 4. As a result of this measurement for the GHZ channel, as shown in Fig. 2(A3), particles 6, 7, and 8 are no longer entangled with GHZ quantum correlation and entanglement between particles 2, 4, and 5 vanishes, while for the cluster-state channel, as shown in Fig. 2(B3), the entanglement between particles 2,

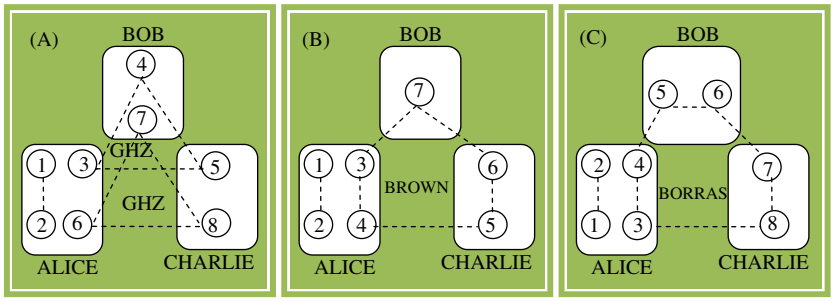

Fig. 1. This figure shows the tripartite schemes for QSTS and teleportation of the two-qubit state from sender Alice to receiver Charlie under the control of a third party who is Bob. Parts (A), (B), and (C) are valid for GHZ/cluster-, Brown-, and Borras-state channels, respectively. The dotted line between particles shows entanglement between them. Particles 1 and 2, which store two-qubit states, for all four channels, are located in Alice's laboratory. The distribution of the remaining particles for each of the four channels is shown in the respective figure for that channel.

4, 5, 6, 7, and 8 vanishes. For both GHZ- and cluster-state channels after the second Bell-state measurement, particles 2 and 6 are projected into one of the four EPR Bell-states, which are denoted by $\varphi_{26}^{(\pm)}$, $\psi_{26}^{(\pm)}$ and particles 4, 5, 7, and 8 get entangled in the four particle entangled state, which is denoted by $|\psi_{4578}\rangle$. In a given teleportation trial for each of the four possible projected Bell-states of particles 1 and 3 there are four possible projected Bell-states of particles 2 and 6, and therefore both for GHZ- and cluster-state channels there are total of 16 ($= 4 \times 4$) possible projected states of particles 4, 5, 7, and 8. With similar reasoning we can show that at the end of the second Bell-state measurement: (a) for both Brown- and Borras-state channels particles 1 and 3 and particles 2 and 4 are, respectively, projected in one of the four equally likely Bell-states $\varphi_{13}^{(\pm)}$, $\psi_{13}^{(\pm)}$ and $\varphi_{24}^{(\pm)}$, $\psi_{24}^{(\pm)}$, and (b) for Brown-state channel particles 5, 6, and 7, and for Borras-state channel particles 5, 6, 7, and 8 are projected into total of 16 equally likely states, which are denoted by $|\psi_{567}\rangle$ and $|\psi_{5678}\rangle$, respectively.

Step 3. For GHZ- and cluster-state channels, we next make two independent single-particle measurements on particles 4 and 7 [5]. These measurements, which are made on the basis $(1/\sqrt{2})(|0\rangle \pm |1\rangle)$ project particles 4 and 7 into either state $|+\rangle$ or $|-\rangle$ with an equal likely probability of 1/2. As shown in Figs. 2(A4) and 2(B4), for both the GHZ- and cluster-state channels after two single-particle measurements particles 4, 5, 8, and 7 become disentangled, particles 4 and 7 become independent particles, and particles 5 and 8 are projected into a new state $|\psi_{58}\rangle$. Corresponding to each of the 16 possible outcomes of state $|\psi_{4578}\rangle$ there are two possible outcomes of state $|\psi_{58}\rangle$. Thus, in a given teleportation trial for GHZ- and cluster-state channels there are total of 32 possible outcomes of state $|\psi_{58}\rangle$, which are equally likely and occur with a probability of 1/32. For the Brown-state channel we make a single-qubit measurement on particle 7 [6]. This measurement is made on the basis of $|0\rangle$ and $|1\rangle$. As a result of this measurement particle 7 can be projected with equal likely probability of 1/2 to either state $|0\rangle$ or state $|1\rangle$ while particles 5 and 6 are projected to one of the 32 possible new states $|\psi_{56}\rangle$ with equal likely probability of 1/32. For the Borras-state channel we make a Bell-state measurement (BSM-3) on particles

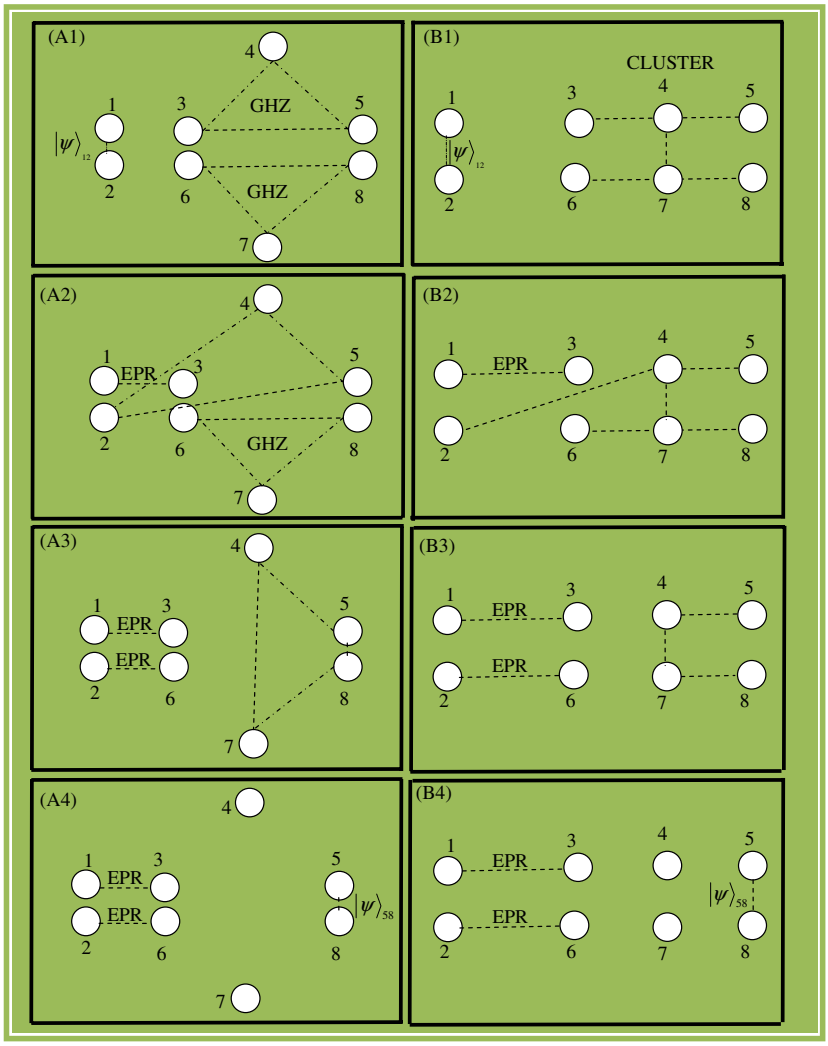

Fig. 2. This figure shows the switching of entanglement among eight quantum particles in a given teleportation trial. Particles connected with dotted lines are entangled. GHZ, Greenberger–Horne–Zeilinger state; EPR, Einstein–Podolsky–Rosen state. Parts (A) and (B) are valid for GHZ- and cluster-state channels, respectively. (A1), (B1) The state of the particles before the first Bell-state measurement. (A2), (B2) The state of the particles after the first Bell-state measurement. (A3), (B3) The state of the particles after the second Bell-state measurement. (A4), (B4) The state of the particles after projecting particles 4 and 7 into a definite quantum state.

5 and 6 [4]. As a result of this measurement particles 5 and 6 can be projected with equal likely probability of 1/4 to one of the four Bell-states: $\varphi_{56}^{(\pm)}$, $\psi_{56}^{(\pm)}$ while particles 7 and 8 are projected to one of the 64 ($=4\times4\times4$) possible new states $|\psi_{78}\rangle$ with equal likely probability of 1/64.

Step 4. To reconstruct the original two-qubit state for all four multipartite channels a unitary transformation (U) is applied on two destination particles in Charlie's laboratory. This transformation, in general, is different for different outcomes and at the location of two destination particles for GHZ-, cluster-, and Borras-state channels is determined by the set of six-binary bits $\{a_1,a_2,a_3,a_4,b_1,b_2\}$, where two binary bits $(a_1a_2)/(a_3a_4)$ represent the projected Bell-state in the first (BSM-1)/second (BSM-2) Bell-state measurement. The two binary bits b_1 and b_2 for GHZ- and cluster-state channels, respectively, represent the projected state of two particles after two single-particle measurements, while for the Borras-state channel they represents the projected Bell-state in the third Bell-state measurement (BSM-3). In a given teleportation trial, each set of six-binary bits $\{a_1,a_2,a_3,a_4,b_1,b_2\}$ correspond to a specific projected state of two destination particles. Note, for the Brown-state channel the corresponding five-binary bits are $\{a_1,a_2,a_3,a_4,b_1\}$. In the case of the GHZ channel, the unitary transformation (U) is applied on two destination particles 5 and 8. This required transformation $U=U_\sigma=U_5\otimes U_8$ [11], where 5 and 8 refers to the two destination qubits. U_5 and U_8 can be written in the terms of identity operator (I) and usual Pauli matrices ($\hat{\sigma_x},\hat{\sigma_y},\hat{\sigma_z}$). Transformation U_5 and U_8 can be applied by the single-qubit operation. In the case of the cluster-state channel, the unitary transformation (U) is also applied on two destination particles 5 and 8. This required transformation (U) consists of two individual transformations, which are (1) U_P and (2) U_σ. The first transformation (U_P) is applied with a two-qubit quantum-controlled phase gate (QCPG), which is followed by a second transformation U_σ. In the case of the Brown-state channel, the unitary transformation (U) is applied on two destination particles 5 and 6. This required transformation (U) consists of three individual transformations, which are U_P, U_N, and U_σ. In this case, the first transformation U_P is followed by second transformation U_N, which is applied with the two-qubit-controlled NOT gate. This second transformation is followed by third transformation U_σ. In the case of the Borras-state channel, the unitary transformation (U) is applied on two destination particles 7 and 8. This required transformation (U) consists of two individual transformations, which are U_N and U_σ. The net result of teleportation after the application of the unitary transformation (U) for all four multipartite channels is the removal of the composite qubit from particles 1 and 2 in Alice's laboratory and its appearance in two destination particles in Charlie's laboratory.

3. EXPERIMENTAL SETUPS FOR QSTS AND TELEPORTATION OF THE TWO-QUBIT PHOTONIC STATE

Tripartite teleportation schemes employing the two-qubit state as discussed in the previous section for GHZ-, cluster-, and Borras- (Brown)-state channels requires a total of eight (seven) identical quantum particles. Our tripartite schemes can be practiced with the technique of cavity quantum electrodynamics (QED) [12,13], but with eight (seven) high-finesse cavities installed in ultrahigh vacuum (UHV) the experimental complexity is very prohibitive. Alternately, one can use eight (seven) ions in the ion trap [14] but the decoherence requires error correction and therefore experimental expenditure is again very prohibitive. On the other hand, photons are the best carrier of information, negligibly affected by decoherence, and are compatible with available fiber telecommunication technology. Thus, our tripartite teleportation schemes can most easily be implemented by using the two-qubit photonic state. A block diagram of the experimental apparatus required for developing the tripartite teleportation system for teleporting the two-qubit photonic state using GHZ- and cluster-state channels is very similar and is shown in Fig. 3. This figure is drawn for the cluster-state channel but after making two changes the same figure is also valid for the GHZ-state channel. The two required changes are

(1) The replacement of the six-photon cluster-state source with a six-photon GHZ-state source, which is shown in the dotted-box inset of Fig. 3. We note that the six-photon GHZ source consists of two independent three-photon GHZ sources.

(2) In Charlie's laboratory for the GHZ channel the QCPG is not required. Therefore, for the GHZ channel this gate needs to be deleted from Fig. 3. Corresponding block diagrams when using Brown- and Borras-state channels are shown in Figs. 4 and 5, respectively. In Figs. 3–5 Alice, Bob, and Charlie are, respectively, sender, controller, and receiver.

In the Alice's laboratory, as shown in Figs. 3–5, a UV pulse excites β-BaB_2O_4(BBO) crystal, which by type II ultrafast spontaneous parametric down-conversion (SPDC) produces a pair of entangled photons that are labeled as 1 and 2 [15]. These two EPR quantum-correlated photons are entangled in their polarization degree of freedom. Photons 1 and 2 are, respectively, transmitted through a combination of wave plates and polarizers $P1$ and $P2$. By adjusting the wave plates and polarizers in the paths of photons 1 and 2 any arbitrary two-qubit entangled photon state $|\psi_{12}\rangle$ to be teleported can be generated. We note, these are not the photons 1 and 2 themselves but rather it is their joint quantum state $|\psi_{12}\rangle$ that Alice wishes to transport to the distinct receiver Charlie!

For creating the GHZ channel, GHZ Source-1 and Source-2 are two separate high-intensity sources of three GHZ entangled photons. Both these sources are pumped by the same UV pulses, which are generated by frequency doubling of the beam from an ultrashort pulse laser, which delivers ≈100 fs light pulses centered near 800 nm and operates at repetition rate of 80 MHz. The laser peak power at 800 nm is >337 kW. The temporal pulse width of this laser can be tuned from ≈35 fs to ≈100 ps. These GHZ sources are based on selecting the three-photon entangled state from the product state of an entangled photon pair and a weak coherent state, which in these GHZ sources is provided by a single-photon pulse [16,17]. The experimentally observed intensity of these GHZ sources is about ≈450 Hz with potential to increase it to ≈1 kHz [17]. The photons generated by Source-1 are labeled as 3, 4, and 5, while 6, 7, and 8 denotes the three GHZ photons generated by Source-2. Genuine GHZ entanglement among three photons generated by the GHZ source can be tested by measuring the expectation value of the entanglement witness operator $W=(1/2)\hat{I}-|\psi\rangle_{ijk}\langle\psi|$. The expectation value

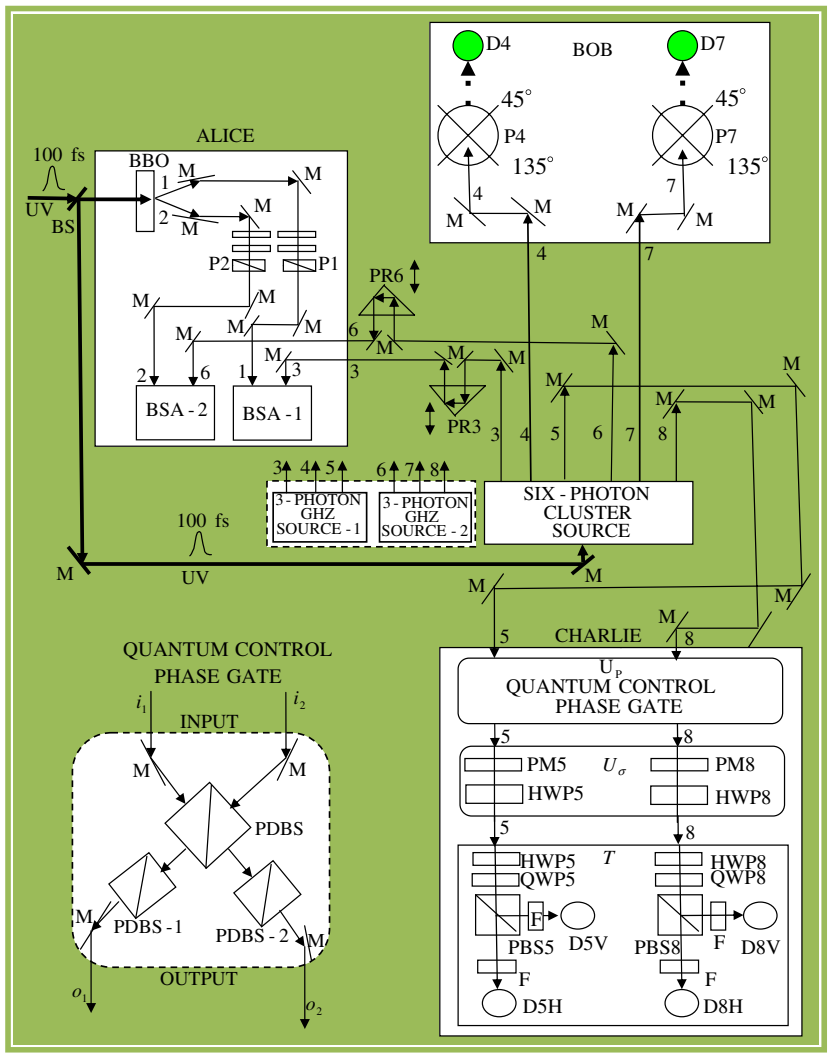

Fig. 3. This figure shows a block diagram of the experimental apparatus required to verify QSTS and quantum teleportation of the two-qubit photonic state from sender Alice to receiver Charlie under the control of Bob. This figure is valid for GHZ- and cluster-state channels. BBO, beta barium borate crystal; M, turning mirror; P1, P2, P4, and P7, linear polarizer; BSA-1 and BSA-2, Bell-state analyzer; PR3 and PR6, time delay prism; UV, ultraviolet 100 fs light pulse; PM5 and PM8, phase modulator; HWP5 and HWP8, half-wave plate; QWP5 and QWP8, quarter-wave plate; PBS5 and PBS8, polarizing beam splitter cube; D4, D7, D5H, D5V, D8H, and D8V, single photon detector; F, narrowband filter; BS, beam splitter; PDBS, polarization-dependent beam splitter cube; PDBS-1 and PDBS-2, polarization-dependent beam splitter.

of entanglement witness operator is $\langle W\rangle = (1/2) - \langle F\rangle$, where, fidelity F is given as $F = \mathrm{Tr}(\rho_{\mathrm{exp}}|\psi_{ijk}\rangle\langle\psi_{ijk}|)$ and ρ_{exp} is the density matrix of the product state. The fidelity can be determined by local measurements on individual qubits. The measured value of the expectation value of the entanglement witness operator for experimentally generated GHZ photons is -0.311 ± 0.002 [17]. This negative value of the expectation value of the entanglement witness operator implies the existence of genuine entanglement among three photons generated by the GHZ source [18] and thus justifies the use of the GHZ channel for developing a tripartite teleportation system. The six-photon cluster state can be experimentally generated by fusion of two-qubit graph-states with the leaf node of a four-qubit star-graph [19,20]. This fusion of two smaller graph-states into a single large graph-state can be experimentally achieved by appropriately combining three pairs of EPR-correlated photons at two polarizing beam splitter (PBS) cubes [21]. In a real experiment each of the three pairs of EPR-correlated photons is generated by the spontaneous parametric down-conversion (SPDC) in the beta barium borate (BBO) crystal. These three pairs are labeled as photons 3 and 4, photons 5 and 6, and photons 7 and 8. To generate the cluster state, photons 4 and 5 and photon 6, which is through a half-wave plate oriented at 22.5°, and photon 7 are precisely overlapped in two different PBS cubes. Photon 3, photon 8, and the outputs of two PBS cubes are detected with single-photon detectors. The multifold coincidence detection of these photons results in the generation of the six-photon cluster state [22]. To test the genuine entanglement of the six-photon cluster state given by Eq. (2) we use the witness $\tilde{W}_C$, which is given as $\tilde{W}_C = (1/2) - |C_6\rangle\langle C_6| + |\tilde{C}_6\rangle\langle\tilde{C}_6|$ [22,23]. The determination of the expectation value of witness $\tilde{W}_C$ requires six measurement settings, which are $\sigma_z^{\otimes 3}\sigma_x^{\otimes 3}$, $\sigma_x^{\otimes 3}\sigma_z^{\otimes 3}$, $\sigma_z^{\otimes 3}M_{(\pm)}^{\otimes 3}$, $M_{(\pm)}^{\otimes 3}\sigma_z^{\otimes 3}$. The experimentally measured value of $\mathrm{Tr}(\tilde{W}_C\rho_{\mathrm{exp}})$ is -0.095 ± 0.036 [22]. This negative value proves the genuine entanglement among six photons generated by the cluster-state source and therefore justifies the use of the cluster-state channel for developing

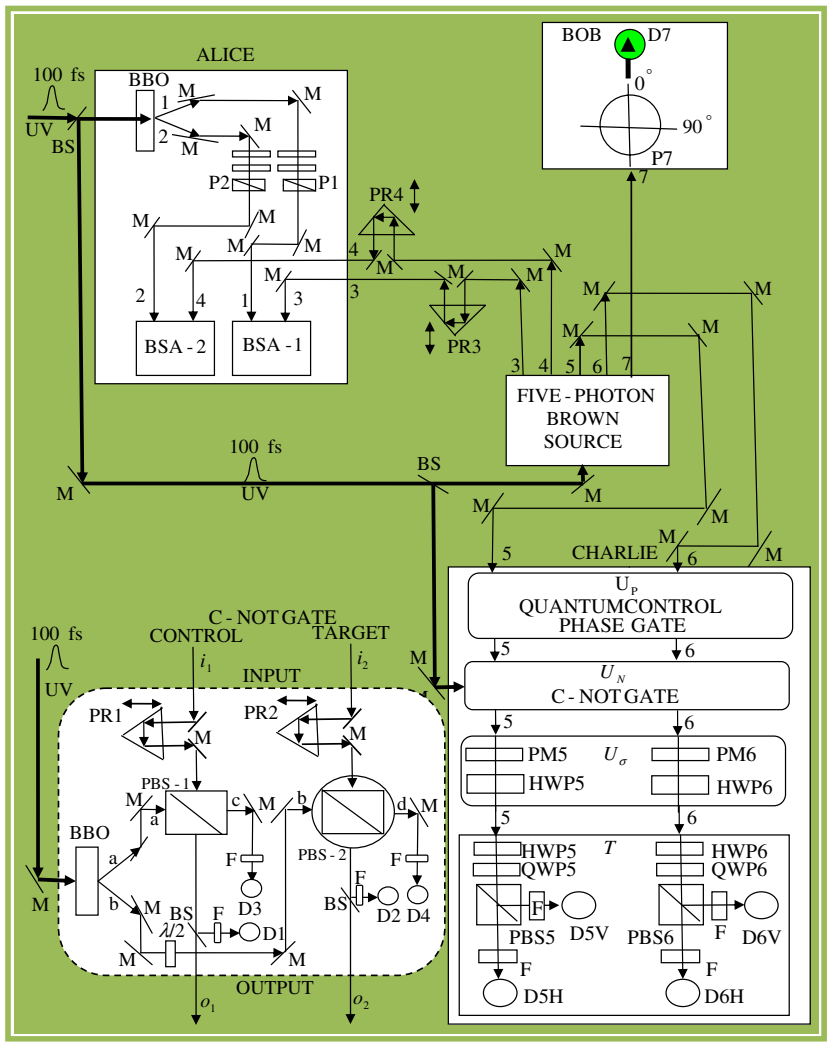

Fig. 4. Description of this figure is very similar to that of Fig. 3 except this figure is valid for the Brown-state channel. Most of the optical components in this figure are same as that in Fig. 3 except for PR1, PR2, and PR4, time delay prism; PM6, phase modulator; HWP6 and $\lambda/2$, half-wave plate; QWP6, quarter-wave plate; PBS6, PBS-1, and PBS-2, polarizing beam splitter cube; D6H, D6V, D1, D2, D3, and D4, single photon detector.

a tripartite teleportation system. The distribution of six photons generated by GHZ- and cluster-state sources to Alice, Bob, and Charlie is shown in Fig. 3. In this distribution, photons 3 and 6, respectively, through time-delay prisms PR3 and PR6 are deflected to Alice's laboratory. Photons 4 and 7 are deflected to Bob while photons 5 and 8 are deflected to Charlie's laboratory. The five-photon Brown state has not yet been experimentally generated and therefore any experimental measurement on the individual qubits of this state is not yet available but negative partial transpose (NPT), von Neumann entropy [9], and multiple entropy (MEMS) [24] measures that this state is genuinely entangled and exhibits more entanglement than GHZ and cluster states. This justifies the use of the five-photon Brown state for tripartite teleportation. The distribution of five-photons generated by the Brown-state source is shown in Fig. 4 and is as follows: photons 3 and 4, respectively, through time delay prisms PR3 and PR4 are deflected to Alice, photon 7 is deflected to Bob, and photons 5 and 6 are deflected to Charlie. To our knowledge experimental demonstration of the Borras state has also not yet been reported but this state exhibits genuine entanglement as concluded by many different measurements [10]. First, it exhibits all the marginal density matrices for the states of one, two, three qubits completely mixed. Second, this state evolves to a mixed state with a higher amount of entanglement than any other state of six-qubits such as the cluster state. Third, entanglement of this state decays more slowly than that of the GHZ state. The very high entanglement content in this state greatly encourages the use of this state for future quantum communication experiments. The distribution of six-photons generated by the Borras-state source is shown in Fig. 5 and is as follows: photon 3 and 4, respectively, through time-delay prisms PR3 and PR4 deflected to Alice, photon 5 through time-delay prism PR5 and photon 6 are deflected to Bob, and photon 7 and 8 are deflected to Charlie.

In Alice's laboratory, as shown in Fig. 3 (Figs. 4 and 5), for GHZ- and cluster- (Brown- and Borras-)state channels photons 1 and 3 and photons 2 and 6 (photons 2 and 4) are, respectively, deflected into Bell-state analyzers (BSA) BSA-1 and BSA-2. The optical setup of the BSA, which is shown in the dotted-box inset of Fig. 5 is discussed elsewhere [25] and the brief description of this setup is as follows. $p1$ and $p2$ are two polarization-entangled photons, which are incident into the Bell-state analyzer. These photons are first processed

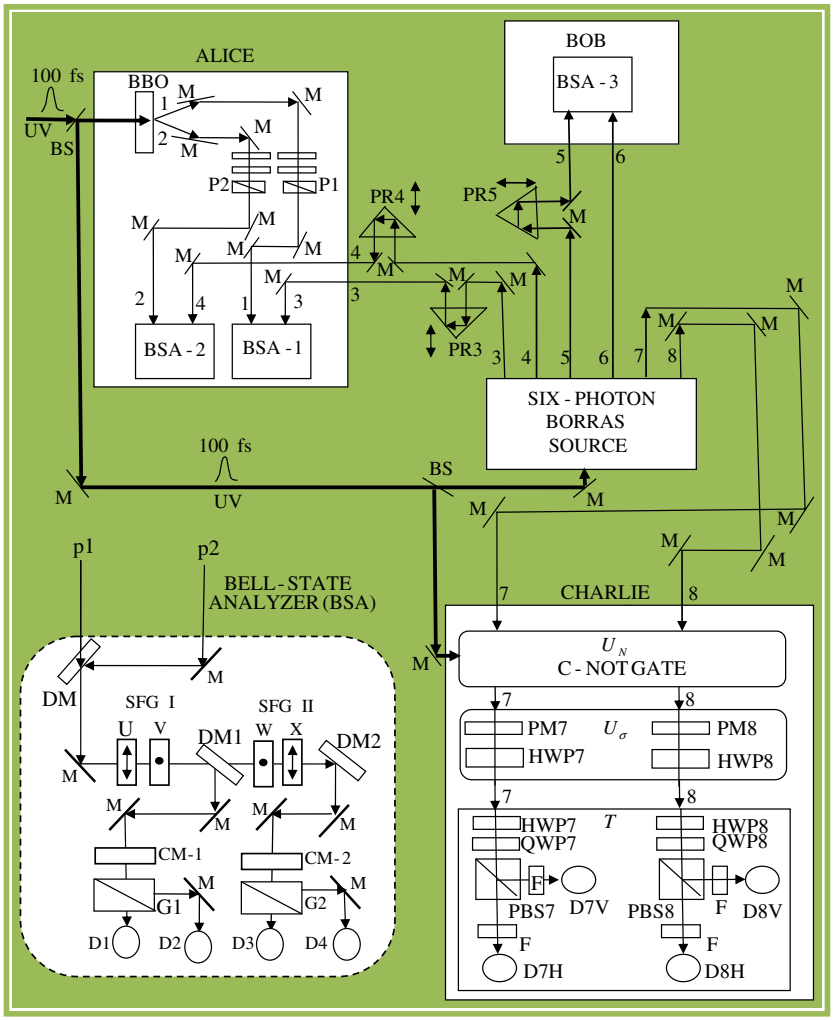

Fig. 5. Description of this figure is very similar to that of Figs. 3 and 4 except this figure is valid for the Borras-state channel. Most of the optical components in this figure are same as that in Figs. 3 and 4 except for BSA-3, Bell-state analyzer; PR5, time delay prism; PM7, phase modulator; HWP7, half-wave plate; QWP7, quarter-wave plate; PBS7, polarizing beam splitter cube; D7H and D7V, single photon detector; DM, DM1, and DM2, dichroic mirror; U, V, W, and X, sum frequency generation (SFG) crystals; CM-1 and CM-2, compensator; G1 and G2, 45° projector; D1, D2, D3, and D4, detectors.

by Type I and Type II sum frequency generation (SFG) nonlinear crystals (U, V, W, X). Then through compensators (CM-1, CM-2) and 45° projectors (G1, G2) are detected at detectors D1–D4. In this Bell-state analyzer, two incident photons can be projected into one of the four Bell-states ($\varphi_{12}^{(+)}$, $\varphi_{12}^{(-)}$, $\psi_{12}^{(+)}$, and $\psi_{12}^{(-)}$), which are, respectively, registered on four detectors D1–D4. For example, a trigger on the detector D_2 indicates that the projected Bell-state of photon $p1$ and photon $p2$ is $\varphi_{12}^{(-)}$. As photons 1 and 2 in the Bell-state analyzers (BSA-1 and BSA-2) are summed by SFG crystals they are lost and therefore the original composite qubit prepared in Alice's laboratory is destroyed. In the Bob's laboratory for GHZ- and cluster-state channels, as shown in Fig. 3, photons 4 and 7 are directed into linear polarizers $P4$ and $P7$, respectively, which can be rotated to either of the two states at 45° or 135°. These two states of the polarizers denote the states $|+\rangle$ and $|-\rangle$, respectively. For the Brown-state channel, as shown in Fig. 4, photon 7 is directed into a linear polarizer $P7$, which can be rotated to either of two states 0° or 90°. These two states of the polarizer denote the states $|0\rangle$ and $|1\rangle$, respectively. For Borras-state channel, as shown in Fig. 5, photons 5 and 6 are directed into a Bell-state analyzer BSA-3. In case of the GHZ channel to apply unitary transformation ($U = U_\sigma$), in the Charlie's laboratory as shown in Fig. 3, photon 5 (8) is transmitted through a combination of a phase modulator (PM5)/(PM8) and a half-wave plate (HWP5)/(HWP8). The Pauli operation σ_z on a photonic state can be realized by transmitting photons through a phase modulator. The Pauli operation σ_x on photonic state can be realized by transmitting photons through a half-wave plate, which is oriented so that its major axis is inclined at an angle $\vartheta = \pi/4$ to the horizontal direction. The Pauli operation $i\sigma_y$ on a photonic state can be realized by transmitting the encoded photon through a phase modulator, which is followed by an appropriately oriented half-wave plate. Therefore, with the combination of a phase modulator and a half-wave plate any of the single-qubit transformations (U_σ) can be experimentally achieved. As shown in Fig. 3 in Charlie's laboratory, after the application of unitary transformation (U_σ) each of the photons 5 and 8 is finally directed into an optical test assembly (T), which is used to verify the final teleported state received in these two destination photons. The optical test assembly consists of a half-wave plate

(HWP) and a quarter-wave plate (QWP), which is followed by a PBS cube. The transmitted photons out of the PBS cube are through a narrowband filter (F) detected by a single-photon detector (D). In case of the cluster-state channel, to apply a unitary transformation (U_P) in the Charlie's laboratory as shown in Fig. 3, photons 5 and 8 are directed into a QCPG. An ideal QCPG is a two-qubit gate, which has two inputs [control (i_1) and target (i_2)] and two outputs (o_1o_2). This gate flips the phase of the target qubit if and only if the logical status of both the control and target qubits are synchronously set to unity. The action of this gate is described as $|00\rangle_{i_1i_2} \rightarrow |00\rangle_{o_1o_2}$, $|01\rangle_{i_1i_2} \rightarrow |01\rangle_{o_1o_2}$, $|10\rangle_{i_1i_2} \rightarrow |10\rangle_{o_1o_2}$, and $|11\rangle_{i_1i_2} \rightarrow -|11\rangle_{o_1o_2}$. Optical setup of the QCPG is shown in the dotted-box inset of Fig. 3. The gate operation is applied in case of a coincidence detection between modes i_1 and i_2. As shown in the dotted-box inset of Fig. 3, two input modes i_1 and i_2 are overlapped in a polarization-dependent beam splitter cube (PDBS). The transmitted beams out of the PDBS from mode i_1 and i_2 are further transmitted through polarization-dependent beam splitters PDBS-1 and PDBS-2, respectively. The beam splitter cube is custom made with dielectric coating specially designed so that it has a transmission coefficient of unity for the horizontal and 1/3 for the vertical state of polarization. PDBS-1 and PDBS-2 are two identical beam splitters, which are also custom designed so that they have a transmission coefficient of unity for the vertical and 1/3 for the horizontal state of polarization. We note, PDBS and PDBS-1/PDBS-2 have a reverse splitting ratio for horizontal and vertical polarizations. In this gate, the phase is introduced by second-order interference of indistinguishable photons in the PDBS [26,27]. The transmission of 1/3 for vertical polarization results in a total amplitude of −1/3 for the $|11\rangle$ output while perfect transmission for horizontal polarization results in no interference contribution for input states $|00\rangle_{i_1i_2}$, $|01\rangle_{i_1i_2}$, and $|10\rangle_{i_1i_2}$. The operation of this gate with a short-pulsed laser has been experimentally verified [27]. As shown in Fig. 3, each of the photons 5 and 8 transmitted out of the QCPG is directed into a combination of the phase modulator and half-wave plate. This is to apply unitary transformation (U_σ). To verify the final teleported state received in photons 5 and 8, these photons are finally directed into the optical test assembly (T). In the case of the Brown-state channel, to apply the unitary transformation (U_P) in Charlie's laboratory as shown in Fig. 4, photons 5 and 6 are first directed into a QCPG. The two outputs of this gate then form the two inputs of a C-NOT gate, which is used to apply unitary transformation (U_N). An ideal C-NOT gate is a two-qubit gate, which has two inputs [control (i_1) and target (i_2)] and two outputs (o_1o_2). This gate flips the logical status of the target qubit if and only if the logical status of the control qubit is set to unity. The action of this gate is described as $|00\rangle_{i_1i_2} \rightarrow |00\rangle_{o_1o_2}$, $|01\rangle_{i_1i_2} \rightarrow |01\rangle_{o_1o_2}$, $|10\rangle_{i_1i_2} \rightarrow |11\rangle_{o_1o_2}$, and $|11\rangle_{i_1i_2} \rightarrow |10\rangle_{o_1o_2}$. The optical setup of the C-NOT gate is shown in the dotted-box inset of Fig. 4. The left part of this optical setup is the quantum encoder while the right part is the destructive C-NOT [28,29]. In the design of this gate a UV pulse excites the BBO crystal producing a pair of entangled photons, which are shown in the dotted-box inset of Fig. 4 and are labeled as photons a and b. Photon b is transmitted through a half-wave plate ($\lambda/2$). Photons a and b are prepared in the EPR-state $\varphi_{ab}^{(+)}$. In the polarization beam splitter cube (PBS-1)/(PBS-2) photon a/b is spatially and temporally overlapped with the control (i_1)/target (i_2) input to the gate, where PBS-2 is rotated by 45°. The two outputs of the polarization beam splitter cube (PBS-1)/(PBS-2), which are denoted by (o_1 and c)/(o_2 and d) are detected with fiber-coupled detectors (D_1 and D_3)/(D_2 and D_4). The function of narrow-banding filters (F) in the front of each of the four detectors $D_1 - D_4$ is to stretch the coherence time of the photon so that it becomes greater than the temporal length of the light pulse. This results in the indistinguishability of the photons upon detection. A fourfold coincidence at the detectors $D_1 - D_4$ results in the C-NOT operation between two input (i_1i_2) and two output (o_1o_2) states of the gate. The operation of this gate with a short-pulsed laser has been experimentally verified [30]. Each of the two outputs of the C-NOT gate is then supplied to the combination of a phase modulator and a half-wave plate, which is used to apply a unitary transformation (U_σ). To verify the final teleported state received in photons 5 and 6, these photons are finally directed into the optical test assembly (T). In the case of the Borras-state channel, to apply a unitary transformation (U_N) in Charlie's laboratory as shown in Fig. 5, photons 7 and 8 are first directed into a C-NOT gate. As shown in Fig. 5, each of the two outputs of the C-NOT gate is next supplied to the combination of a phase modulator and a half-wave plate, which is used to apply unitary transformation (U_σ). To verify the final teleported state received in photons 7 and 8 these photons are finally directed into the optical test assembly.

The demonstration procedure for teleportation of the two-qubit photonic state from Alice to Charlie proceeds in following steps. For each of the four multipartite channels, Alice in her laboratory prepares various different composite qubits in photons 1 and 2. In the case of the GHZ- and cluster- (Brown- and Borras-)state channels, with prisms PR3 and PR6 (PR4) Alice first adjusts the time-delays so that photons 1 and 3 and photons 2 and 6 (2 and 4) exactly overlap in the SFG crystal inside the Bell-state analyzers and then determines the projected Bell-states of photons 1 and 3 and photons 2 and 6 (2 and 4). After the Bell-state measurements in Alice's laboratory, Bob, in the case of GHZ- and cluster-state channels, rotates both his polarizers either to state $|+\rangle$ or to state $|-\rangle$. In the case of the Brown-state channel, Bob rotates his polarizer either to state $|0\rangle$ or to state $|1\rangle$. In the case of the Borras-state channel, Bob adjusts the time delay with prism PR5 and determines the projected Bell-state of photons 5 and 6. After Bob completes his measurements, Charlie, in the case of each of the four multipartite channels with optical test assembly (T), analyzes the projected state of the two destination particles. Repeated matches between the two-qubit state prepared in Alice's laboratory and the experimentally analyzed two-qubit state in Charlie's laboratory with fidelity greater than the classical fidelity of 2/3 prove the faithful teleportation of an arbitrary two-qubit photonic state from Alice's to Charlie's laboratory.

4. COMPARISON AMONG MULTIPARTITE QUANTUM CHANNELS AND EXPERIMENTAL DIFFICULTIES

In this paper, we have considered a pair of three-photon GHZ, six-photon cluster, five-photon Brown, and six-photon Borras states. The entanglement structure of these multipartite states is different. As a result, these states exhibit different physical

properties and results in different efficiencies when used in the same quantum communication protocol. Entanglement in the cluster state is more persistent than in the GHZ state and further, the cluster state is more robust against decoherence than the GHZ state. For the GHZ state NPT measure $E_{\mathrm{NPT}}|\psi_{\mathrm{GHZ}}\rangle = 1.5$, while for the Brown state $E_{\mathrm{NPT}}|\psi_5\rangle = 17.5$. Von Neumann entropy for the GHZ state is 1 for every cut while for the Brown state it is 2 for two-index cuts [9]. Thus, the Brown state, both by NPT and von Neumann entropy, measure is far more highly entangled than the GHZ state. As concluded by four alluded measures, which are linear entropy (E_L), von Neumann entropy (E_{VN}), Renyi entropy (E_R), and negativity (E_N), the six-photon Borras state in comparison to the GHZ, cluster, and Brown states exhibit very high entanglement [10]. In addition, entanglement in the Borras state decays more slowly than in the GHZ state and is more robust against depolarizing channels [4].

Tripartite teleportation schemes, their hardware implementation, and teleportation procedure for four different multipartite channels appear the same but differ in their individual steps. Schemes for GHZ- and cluster-state channels are very similar but are different from the schemes for Brown- and Borras-state channels. Schemes for Brown- and Borras-state channels are also different from each other. The major difference among the scheme, their hardware implementation, and teleportation procedure lies in

(a) The multiphoton entangled state source used in the experimental apparatus.
(b) Distribution of entangled photons from the source to Alice, Bob, and Charlie's laboratories.
(c) The total number of entangled photons required to experimentally practice the scheme. Experimentation using GHZ-, cluster-, and Borras-state channels requires 6 but the Brown-state channel requires only five entangled photons.
(d) Individual measurements performed in Alice, Bob, and Charlie's laboratories. The difference in such measurements is especially apparent in Bob and Charlie's laboratories.

Among the major difficulties for the experimental demonstration is the unavailability of high-intensity entangled photon sources of multipartite entangled states. Three-photon GHZ- and six-photon cluster-state sources have been experimentally demonstrated [17,22,31]. The photon flux of these sources is very low but can be increased by replacing the BBO with a quasi-phase-matched periodically poled nonlinear crystal [32,33], which has higher nonlinear susceptibility than that of BBO. The five-photon Brown state given by Eq. (3) has not yet been experimentally generated, but as suggested in [3] can be experimentally realized as follows. We consider five identical photons, which are labeled as 3, 4, 5, 6, and 7. Photons 3 and 4 and photons 6 and 7 are, respectively, prepared in the maximally entangled EPR-Bell-state $\psi_{34}^{(+)}$ and $\varphi_{67}^{(+)}$ while photon 5 is prepared in the state $|+\rangle_5 = (1/\sqrt{2})(|0\rangle_5 + |1\rangle_5)$. Then the first three-photon W-class state can be generated by performing a two-qubit C-NOT (4,5) operation on the combined state of photons 3, 4, and 5. Finally, the five-photon Brown state can be generated by performing a unitary operation on the combined state consisting of the W-state of photons 3, 4, and 5 and the Bell-state of photons 6 and 7. The six-photon Borras state has total of 32 superposition terms, which are displayed in Eq. (4). Due to the very large number of superposition terms, this highly entangled state is very hard to experimentally generate. This state can be experimentally realized by first creating three pairs of EPR-correlated photons in periodically poled nonlinear crystals. These six-photons can be further appropriately combined in the PBS cubes. Finally, the six-photon Borras state can be generated by subsequent C-NOT and Hadamard operations followed by multifold coincidence detection. Another major difficulty is the SFG in the Bell-state analyzers, which is required for complete Bell-state measurements. Due to the low photon flux, the nonlinear interaction in these Bell-state analyzers occurs in few photon regimes and therefore the strength of the underlying nonlinear interaction is very weak. Such weak nonlinear interaction can be enhanced by matching the spatial length of the light pulse to the physical length of the nonlinear crystal [34]. The imperfections in the QCP and C-NOT gates, which are required for unitary transformation (U) constitute another difficulty in the experimental demonstration. Such imperfections can degrade the fidelity and the success probability of the teleported two-qubit photonic state.

5. REMARKS

The whole result of this paper can simply be put as follows: subjected to the availability of a multipartite entangled photon source and with enough photon flux, the QSTS and the perfect teleportation of the two-qubit photonic state, using any of the four multipartite quantum channels considered in this paper, can be experimentally demonstrated. The experiment discussed in this paper can be extended to demonstrate tripartite quantum communication photonic networks, in which the two-qubit state can be teleported from any node to any other node in the network [35]. The experimental techniques and methods discussed in this paper can be used to demonstrate other related protocols, such as quantum dense coding [36] and remote state preparation [37,38] using genuinely entangled multipartite states.

REFERENCES

1. A. Karlsson and M. Bourennane, "Quantum teleportation using three-particle entanglement," Phys. Rev. A **58**, 4394–4400 (1998).
2. N. Paul, J. V. Menon, S. Karumanchi, S. Muralidharan, and P. K. Panigrahi, "Quantum tasks using six qubit cluster states," Quant. Info. Proc. **10**, 619–632 (2011).
3. S. Muralidharan and P. Panigrahi, "Perfect teleportation, quantum-state sharing, and superdense coding through genuinely entangled five-qubit state," Phys. Rev. A **77**, 032321 (2008).
4. S. Choudhury, S. Muralidharan, and P. K. Panigrahi, "Quantum teleportation and state sharing using a genuinely entangled six-qubit state," J. Phys. A **42**, 115303 (2009).
5. Y. Li and K. Hou, "Tripartite controlled teleportation of an arbitrary two-qubit state with multipartite cluster states," Int. J. Quantum. Inform. **08**, 969–977 (2010).
6. K. Hou, Y. Li, and S. Shi, "Quantum state sharing with genuinely entangled five-qubit state and Bell-state measurements," Opt. Commun. **283**, 1961–1965 (2010).
7. D. M. Greenberger, M. A. Horne, and A. Zeilinger, "Going beyond Bell's theorem" in *Bell's Theorem, Quantum Theory and Conceptions of the Universe*, M. Kafatos, ed. (Kluwer Academic, 1989), pp. 73–76.
8. H. J. Briegel and R. Raussendorf, "Persistent entanglement in arrays of interacting particles," Phys. Rev. Lett. **86**, 910–913 (2001).
9. I. D. K. Brown, S. Stepney, A. Sudbery, and S. L. Braunstein, "Searching for highly entangled multi-qubit states," J. Phys. A **38**, 1119–1131 (2005).

10. A. Borras, A. R. Plastino, J. Batle, C. Zander, M. Casas, and A. Plastino, "Multiqubit systems: highly entangled states and entanglement distribution," J. Phys. A **40**, 13407–13421 (2007).
11. G. Rigolin, "Quantum teleportation of an arbitrary two-qubit state and its relation to multipartite entanglement," Phys. Rev. A **71**, 032303 (2005).
12. H. J. Kimble, "Strong interactions of single atoms and photons in cavity QED," Phys. Scr. **T76**, 127–137 (1998).
13. H. Mabuchi, J. Ye, and H. J. Kimble, "Full observation of single-atom dynamics in cavity QED," Appl. Phys. B **68**, 1095–1108 (1999).
14. R. Blatt and D. Wineland, "Entangled states of trapped atomic ions," Nature **453**, 1008–1015 (2008).
15. P. G. Kwiat, K. Mattle, H. Weinfurter, A. Zeilinger, A. V. Sergienko, and Y. Shih, "New high-intensity source of polarization-entangled photon pairs," Phys. Rev. Lett. **75**, 4337–4341 (1995).
16. J. G. Rarity and P. R. Tapster, "Three-particle entanglement from entangled photon pairs and a weak coherent state," Phys. Rev. A **59**, R35–R38 (1999).
17. H. Lu, J. Zhang, X. Wang, Y. Li, and C. Wang, "Experimental high-intensity three-photon entangled source," Phys. Rev. A **78**, 033819 (2008).
18. M. Bourennane, M. Eibl, C. Kurtsiefer, S. Gaertner, H. Weinfurter, O. Guhne, P. Hyllus, D. Bru, M. Lewenstein, and A. Sanpera, "Experimental detection of multipartite entanglement using witness operators," Phys. Rev. Lett. **92**, 087902 (2004).
19. M. Hein, J. Eisert, and H. J. Briegel, "Multiparty entanglement in graph states," Phys. Rev. A **69**, 062311 (2004).
20. D. E. Browne and T. Rudolph, "Resource-efficient linear optical quantum computation," Phys. Rev. Lett. **95**, 010501 (2005).
21. T. P. Bodiya and L. M. Duan, "Scalable generation of graph-state entanglement through realistic linear optics," Phys. Rev. Lett. **97**, 143601 (2006).
22. C. Lu, X. Zhou, O. Guhne, W. Gao, J. Zhang, Z. Yuan, A. Goebel, T. Yang, and J.-W. Pan, "Experimental entanglement of six photons in graph states," Nat. Phys. **3**, 91–95 (2007).
23. G. Toth and O. Guhne, "Entanglement detection in the stabilizer formalism," Phys. Rev. A **72**, 022340 (2005).
24. D. Liu, X. Zhou, and G. L. Long, "Multiple entropy measures for multipartite quantum entanglement," arXiv:0705.3904 (2007).
25. Y. Kim, S. P. Kulik, and Y. Shih, "Quantum teleportation of a polarization state with a complete Bell-state measurement," Phys. Rev. Lett. **86**, 1370–1373 (2001).
26. H. F. Hofmann and S. Takeuchi, "Quantum phase gate for photonic qubits using only beam splitters and postselection," Phys. Rev. A **66**, 024308 (2002).
27. N. Kiesel, C. Schmid, U. Weber, R. Ursin, and H. Weinfurter, "Linear optics controlled-phase gate made simple," Phys. Rev. Lett. **95**, 210505 (2005).
28. T. B. Pittman, B. C. Jacobs, and J. D. Franson, "Probabilistic quantum logic operations using polarizing beam splitters," Phys. Rev. A **64**, 062311 (2001).
29. T. B. Pittman, B. C. Jacobs, and J. D. Franson, "Demonstration of nondeterministic quantum logic operations using linear optical elements," Phys. Rev. Lett. **88**, 257902 (2002).
30. S. Gasparoni, J. W. Pan, P. Walther, T. Rudolph, and A. Zeilinger, "Realization of photonic controlled-NOT gate sufficient for quantum computation," Phys. Rev. Lett. **93**, 020504 (2004).
31. D. Bouwmeester, J. W. Pan, M. Daniell, H. Weinfurter, and A. Zeilinger, "Observation of three-photon Greenberger–Horne–Zeilinger entanglement," Phys. Rev. Lett. **82**, 1345–1349 (1999).
32. M. M. Fejer, G. A. Magel, D. H. Jundt, and R. L. Byer, "Quasi-phase matched second harmonic generation: tuning and tolerances," IEEE J. Quantum Electron. **28**, 2631–2654 (1992).
33. K. Banaszek, A. B. U'Ren, and I. A. Walmsley, "Generation of correlated photons in controlled spatial modes by downconversion in nonlinear waveguides," Opt. Lett. **26**, 1367–1369 (2001).
34. S. E. Harris and L. V. Hau, "Nonlinear optics at low light levels," Phys. Rev. Lett. **82**, 4611–4614 (1999).
35. H. Yonezawa, T. Aokl, and A. Furusawa, "Demonstration of a quantum teleportation network for continuous variables," Nature **431**, 430–433 (2004).
36. P. S. Bhatia, "Controlled quantum dense coding using six-photon cluster state," submitted for publication.
37. X. Chen, S. Ma, Y. Su, R. Zhang, and Y. Yang, "Controlled remote state preparation of arbitrary two and three qubit states via the Brown state," Quant. Info. Proc. **11**, 1653–1667 (2012).
38. M. Luo, J. Peng, and Z. Mo, "Joint remote preparation of an arbitrary five-qubit Brown state," Int. J. Theor. Phys. **52**, 644–653 (2013).